

Dantec 3D Image Correlation System as a Tool for Determining Strength Properties

T. DOMAŃSKI^{a,*}, M. KUBIAK^a,
W. PIEKARSKA^b AND Z. SATERNUS^a

^a Czestochowa University of Technology, 42-201 Czestochowa, Poland

^b University of Technology, 40-555 Katowice, Poland

Doi: [10.12693/APhysPolA.139.539](https://doi.org/10.12693/APhysPolA.139.539)

*e-mail: domanski@imipkm.pcz.pl

The presence of a notch has a decisive influence on the deterioration of the operational properties of each type of construction material. The shape of the notch and the stress distribution in the notch have an influence, in particular with high strains, on the properties of the material tested. To evaluate these properties, the static characteristics of the test material were determined for various notches. The work presents the research possibilities offered by the multi-camera 3D image correlation system. The experiment is based on non-contact measurement of displacements and deformations of axially loaded samples. The samples are made of aluminum AW-1050A. The measurement was mainly used to estimate the value of deformations and displacements at various points of the loaded cross-section. The measurement was performed by following the displacements of the properly prepared outer surface of the sample.

topics: image correlation system 3D, tensile test, deformation, displacement

1. Introduction

The use of a non-invasive measurement method makes it possible to detect defects more quickly without the need for specialist preparation of test specimens. The advantage of using optical measurement methods of deformation or stress distribution is the ability to identify changes in the surface of the test material at the microscale level. This allows early identification of the process before its dynamic development [1].

The Q-400 system used with the ISTR 4D software is a multifunctional non-contact tool for measuring the deformation of a tested object in both two- and three-dimensional coordinate systems. The principles of the system are based on relationships existing in the continuous mechanics. Dimensions and positions of the two points in the state before and after the deformation are considered. The correct operation of the system is based on the appropriate lighting and then the analysis of the light beam reflected from the surface of the observed piece before the load and in the subsequent steps of the load for the consequence deformations to appear. The digital image correlation method used images of the object taken at the same time by several optical cameras with high sensitivity to deformation and vibration of the object being observed. This method of measurement is currently used increasingly to determine the components of stresses, deformations or displacements in

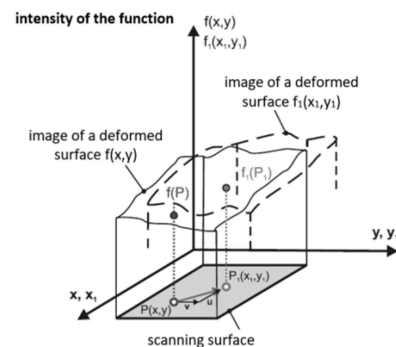


Fig. 1. Diagram of surface image analysis before and after deformation [2].

laboratory conditions, and to identify defects in machine construction components under the influence of static loads or dynamic variables over time [1, 3]. Measurement methods allow for easier adaptation to the measurement of machine parts in their natural industrial environment under real operating conditions.

The correlation algorithm tracks the position of the same points in the source image and the distorted image (Fig. 1). To achieve this square surface containing a set of pixels, it is identified in the source image and in the position corresponding to the image after the deformation. There are many parameters that affect the accuracy of the results. They concern, among other things, the size

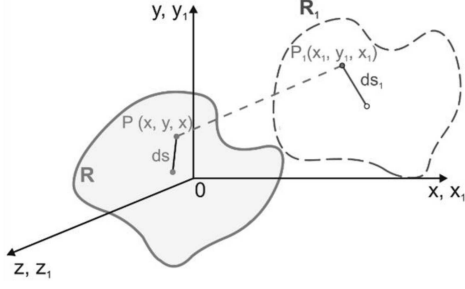


Fig. 2. Characteristic values before (R) and after (R_1) deformation [4].

of the tracked spots, their density, the type of algorithm, the size and the overlap of the set points, etc. [5]. Well-optimized input parameters allow to obtain very accurate results.

The principle of the digital image correlation system is lighting and analysis of the intensity of light that is reflected from the surface in the state before $f(x, y)$ and after deformation $f_1(x_1, y_1)$. In this way, deformation measurement is carried out for small surfaces to finally obtain deformations of the actual surface of the object.

The concept of the digital image correlation method is based on the principles of continuum mechanics. The changes that occur in the dimensions and position of small linear sections between the two points in the initial (P, Q) and deformed (P_1, Q_1) states are analyzed (Fig. 2).

$$P_1 = (x_1, y_1, z_1) = (x + u(P), y + v(P), z + w(P)) \quad (1)$$

$$Q_1 = (x_1 + dx_1, y_1 + dy_1, z_1 + dz_1) = (x + u(P) + u(Q) - u(P) + dx, y + v(P) + v(Q) - v(P) + dy, z + w(P) + w(Q) - w(P) + dz) \quad (2)$$

where u, v, w represent the displacements in the direction of the axis, respectively x, y, z .

The length of the sections is determined using

$$|PQ|^2 = (ds)^2 = dx^2 + dy^2 + dz^2 \quad (3)$$

$$|P_1Q_1|^2 = (ds_1)^2 = dx_1^2 + dy_1^2 + dz_1^2. \quad (4)$$

As a result of using (3) and (4), mathematical transformations become the deformation state components, i.e.,

$$\varepsilon_{xx} \cong \frac{du}{dx} + \frac{1}{2} \left[\left(\frac{\partial u}{\partial x} \right)^2 + \left(\frac{\partial v}{\partial x} \right)^2 \right] \quad (5)$$

$$\varepsilon_{yy} \cong \frac{dv}{dy} + \frac{1}{2} \left[\left(\frac{\partial u}{\partial y} \right)^2 + \left(\frac{\partial v}{\partial y} \right)^2 \right] \quad (6)$$

$$\varepsilon_{xy} \cong \frac{1}{2} \left(\frac{\partial u}{\partial y} + \frac{\partial v}{\partial x} \right) + \frac{1}{2} \left[\frac{\partial u}{\partial x} \frac{\partial u}{\partial y} + \frac{\partial v}{\partial x} \frac{\partial v}{\partial y} \right]. \quad (7)$$

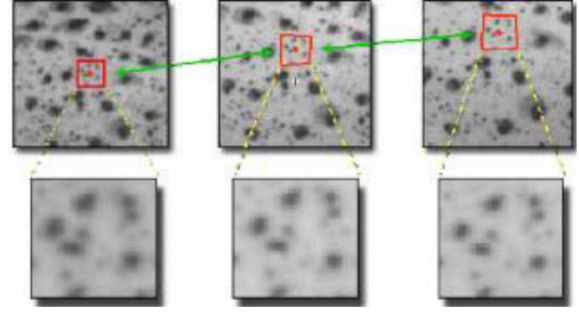


Fig. 3. View of a sample surface [6].

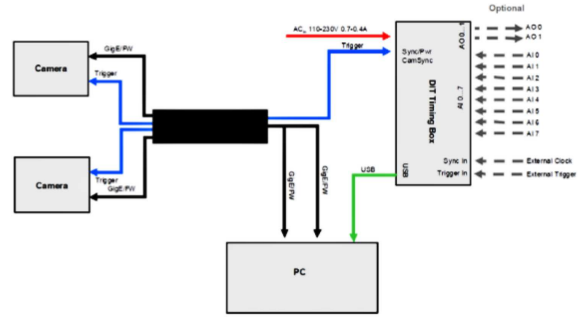


Fig. 4. Connection diagram of the measuring system [7].

The surface of the test object is covered with a layer of white and black paint. The measurement is carried out by tracing the spot surface of the object under load.

Using two digital cameras, it is possible to perform a three-dimensional analysis. When cameras record the examined object from different sides, the position of each point of the object is focused on a specific point of the camera matrix. The position of each point of the examined object in the three-dimensional coordinate system can be calculated when all recording parameters and the focal lengths of the lenses are known, and when the position of both cameras is mutual. In this way, each point on the surface of the test object, tracked by both cameras, can be determined in all planes. Algorithms allow to correlate the same point of the object plane on all cameras used for the study [4, 6, 8].

Object deformation is determined by observing the image recorded with a CCD camera. Correlation algorithms make it possible to determine the maximum displacement with an accuracy of 1/100 of a pixel of the matrix. The correlation algorithm tracks the position of the same points visible in the source image and the distorted image. To achieve this, a square surface containing a set of pixels is identified in the source image and at a position appropriate for the image after deformation (Fig. 3).

There are many parameters that affect the accuracy of the results. They concern, *inter alia*, the size of the tracked spot, its density, the type of algorithm, the size of the point set, overlapping

of the point set, etc. Well-optimized input parameters make it possible to obtain very accurate results [9, 10].

2. Experimental research

A tensile test is one of the basic tests to determine the mechanical properties of materials. The conditions of tensile testing are included in the PN-EN 10002-1. The research uses a universal testing machine Zwick&Roell Z100 with maximum load 100 kN and precision 1 N force/0.01 mm displacement (without a touch extensometer, Fig. 4). Optical cameras used to record strains in the tension test are equipped with 50 mm lenses and have maximum resolution 2048 × 2048 pixels each. This allowed determining the full size of the analyzed sample in the working area of the universal testing machine. A system of three cameras is used in the experiment. The cameras are mounted on the beam which is supported by two fully adjustable tripods (Fig. 5). Strain fields are measured for the entire tension cycle. The trigger mechanism is created in the Istra4D software for the measurement. Pictures are made for every time increment $\Delta t = 0.1$ s.

The samples were made of AW-1050A aluminum, which is characterized by high plasticity and good corrosion resistance. It is susceptible to cold forming, it is not suitable for machining and it is well weldable and sensitive to anodizing. The chemical composition of the aluminum alloy is given in Table I.

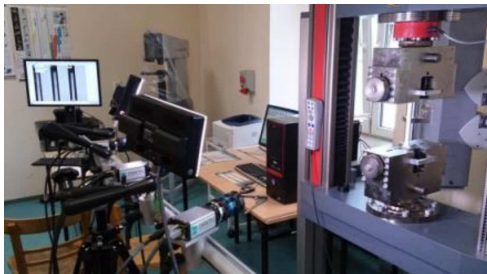


Fig. 5. Tension test: universal strength machine Zwick&Roel Z100, with the Dantec system.

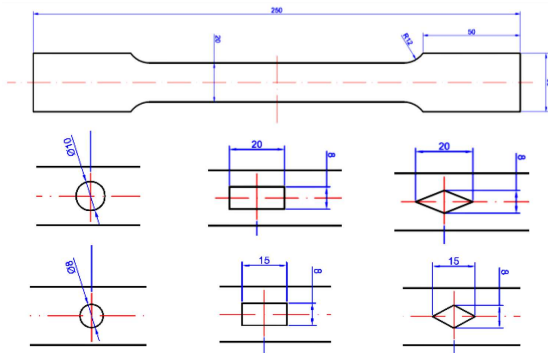


Fig. 6. Geometry of samples.

Chemical composition.

TABLE I

Mg [%]	Mn [%]	Fe [%]	Si [%]	Cu [%]	Zn [%]	Ti [%]
≤ 0.05	≤ 0.05	≤ 0.40	≤ 0.25	≤ 0.05	≤ 0.07	≤ 0.05

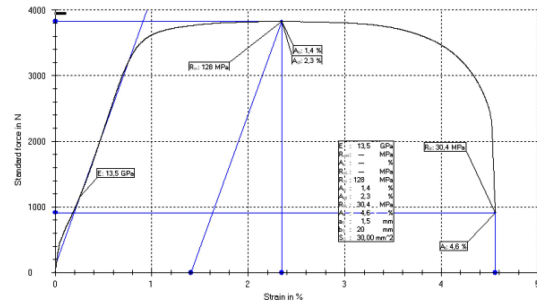


Fig. 7. Tension graph.

Flat samples made of 1.5 mm thick sheet metal with holes of various geometries cut out were prepared for the tests (Fig. 6). The openings are symmetrical in the shape of a rectangle, rhombus and circle.

The relationship between stresses and deformations were determined for a solid flat sample and the most important strength parameters were determined (Fig. 7).

3. Research results

Figure 8 shows the distribution of longitudinal displacements along the measuring length of the full sample. The greatest displacements occur in the upper part of the measuring section. In the following Figs. 9 and 10, the constriction in the smallest cross-section is very clearly visible. The crack formation is visible in the middle of the measuring section.

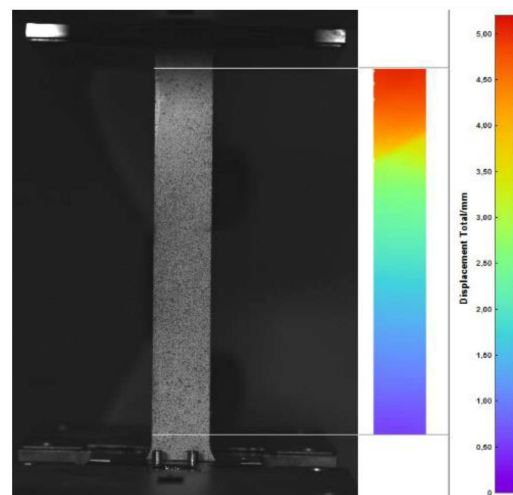


Fig. 8. Distribution of displacement in a sample without a hole.

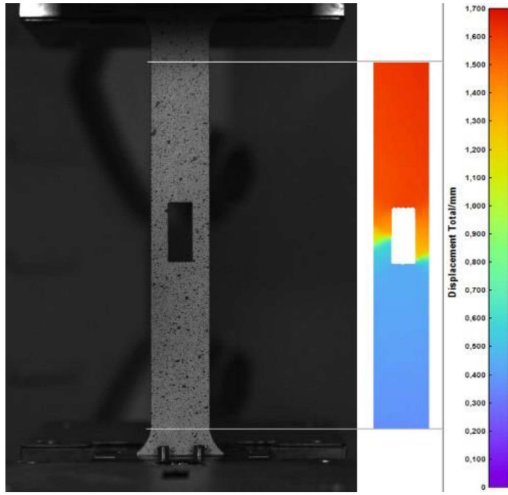


Fig. 9. Distribution of displacement in a sample with a rectangle hole.

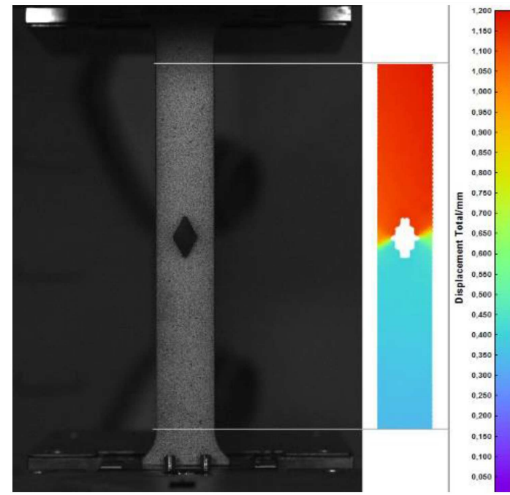


Fig. 12. Distribution of displacement in a sample with a rhombus hole.

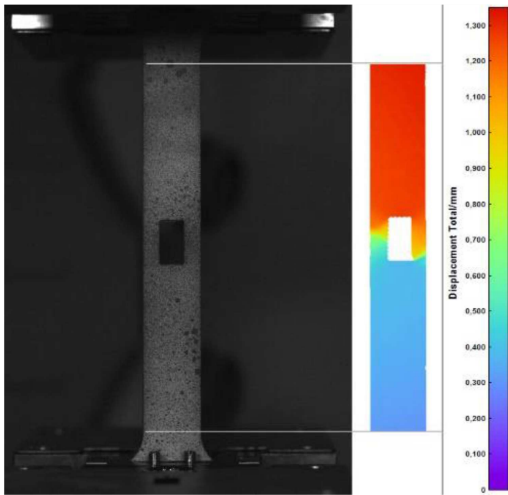


Fig. 10. Distribution of displacement in a sample with a rectangle hole.

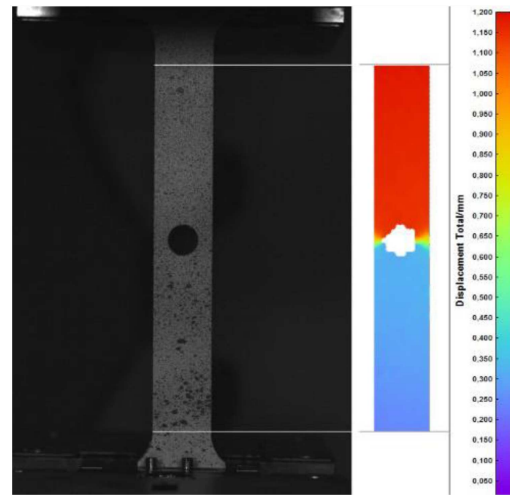


Fig. 13. Distribution of displacement in a sample with a circle hole.

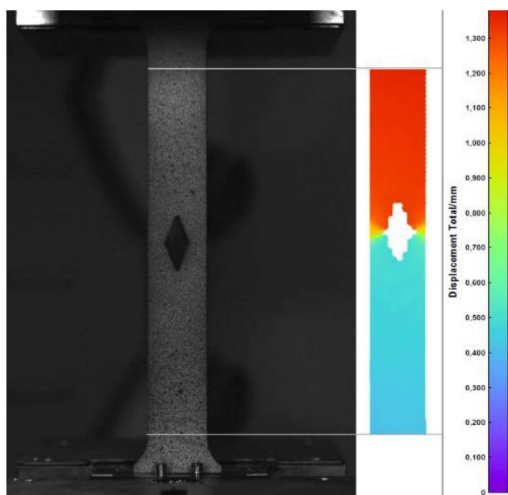


Fig. 11. Distribution of displacement in a sample with a rhombus hole.

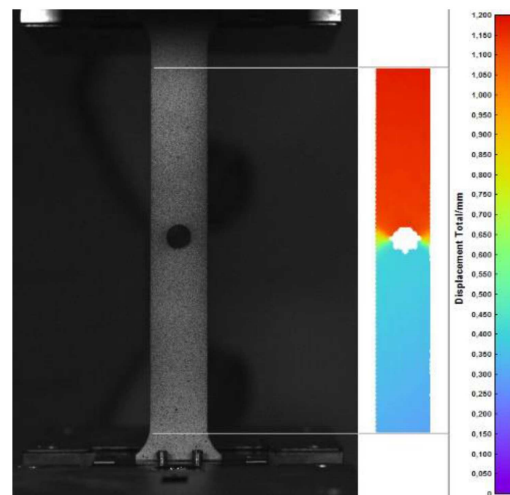


Fig. 14. Distribution of displacement in a sample with a circle hole.

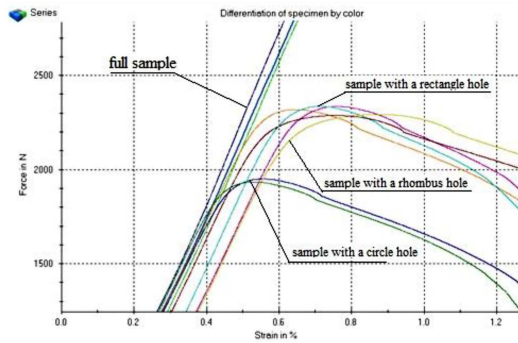


Fig. 15. Tensile diagram, transition to plastic state.

Figures 11 and 12 show cracks in the tops of the rhombus-shaped hole. Figures 13 and 14 demonstrate the displacement distributions of samples with a circular hole. The crack propagation begins in the smallest cross-section. Figure 15 shows the tensile diagrams and the yield stress for all performed tests. For the full sample, the yield point was exceeded at a force of about 3700 N while for the remaining samples with holes at the force from 1800 N to 2300 N.

4. Conclusions

The use of the Dantec Dynamics measuring system allowed for the analysis of displacements in all directions during the rod axial tension test. The system allowed for a very accurate marking of the throat and the line of the crack.

The obtained results may constitute a database for the experimental verification of mathematical and numerical models of the predicted displacements of the axially tensioned rod.

References

- [1] M. Scholze, S. Safavi, K.Ch. Li, B. Ondruschka, M. Werner, J. Zwirner, N. Hammer, *HardwareX* **8**, e00159 (2020).
- [2] T. Szymczak, P. Grzywna, Z.L. Kowalewski, *Transport Samochodowy* **2013**, 79 (2013).
- [3] C. Herbst, K. Splitthof, *Basic of 3D Digital Image Correlation*, Dantec Dynamics, Ulm.
- [4] M. Palanca, L. Cristofolini, *Int. Biomech.* **3**, 1 (2016).
- [5] J.D. Lord, *Digital Image Correlation (DIC), Modern Stress and Strain Analysis. A State of the Art Guide to Measurement Techniques*, 2009, p. 14.
- [6] L. Yang, L. Smith, A. Gotheekar, X. Chen, "Measure Strain Distribution Using Digital Image Correlation (DIC) for Tensile Tests", Final Report, 2010.
- [7] K. Patorski, *Interferometria laserowa*, Oficyna Wydawnicza Politechniki Warszawskiej, 2005, p. 214.
- [8] M. Wojtaszek, T. Sleboda, A. Czulak, G. Weber, W.A. Hufenbach, *Arch. Metall. Mater.* **458**, 1261 (2013).
- [9] T.C. Chu, W.F. Ranson, M.A. Sutton, W.H. Peters, *Exp. Mech.* **25**, 232 (1985).
- [10] M.R. Gower, R.M. Shaw, *Appl. Mech. Mater.* **24–25**, 115 (2010).